Proceeding Paper

Immobilization of Fungal Peroxidase on Paramagnetic Nanoparticles for Synthetic Dye Decolorization †

Kingsley O. Omeje [1],*, Chinonso Magbo [1], Emmanuel C. Ossai [1], Juliet N. Ozioko [1], Benjamin O. Ezema [1], Nonso E. Nnolim [2] and Sabinus O. O. Eze [1]

[1] Department of Biochemistry, University of Nigeria, Nsukka 410001, Enugu State, Nigeria
[2] Applied and Environmental Microbiology Research Group (AEMREG), Department of Biochemistry and Microbiology, University of Fort Hare, Alice 5700, South Africa
* Correspondence: kingsley.omeje@unn.edu.ng
† Presented at the 3rd International Online-Conference on Nanomaterials, 25 April–10 May 2022; Available online: https://iocn2022.sciforum.net/.

Abstract: Peroxidase was produced by *Aspergillus flavus* KIGC on the 11th day of fermentation when grown on banana peel as the sole carbon source. It was purified 8.86-fold with a percentage of recovery of 49.72%. The purified peroxidase was immobilized on magnetic nanoparticles and characterized using DLS, DSC, XRD, FTIR, and SEM analyses. The results suggested an adequate nanoparticle formulation and an effective enzyme immobilization. The optimal temperatures for free and immobilized peroxidase were 75 and 70 °C, respectively; an optimum pH of 5.0 and 9.0 was obtained for the free enzyme and 6.5 and 9.0 for the immobilized peroxidase, respectively. A K_m of 0.075 mM and a catalytic efficiency of 90.66 Mol/S-1 were achieved by the immobilized peroxidase on guaiacol as the substrate. The immobilized peroxidase exhibited enhanced synthetic dye decolorization ability.

Keywords: oxidoreductase; dye decolorization; peroxidase; immobilization; bioremediation

1. Introduction

The high cost of commercial peroxidase and the high rate of its denaturation as a result of unstable conditions regarding temperature, pH, and organic solvents are some of the major challenges facing industrialists and other users. Furthermore, decreases in enzyme activity and the inability to recover and reuse the enzyme are some problems encountered during industrial uses of enzymes. However, enzyme immobilization on some sort of support aids in overcoming these challenges [1]. The most common materials used in enzyme immobilization include silica, chitosan, clay, and polystyrene [1,2]. Currently, enzyme immobilization on nanoparticles is receiving attention from researchers [3–5], due to the attendant advantages it confers to enzymes such as the improvement of their thermal and mechanical property [6]. Furthermore, enzyme activity and stability improve after immobilization [7]. The immobilization of enzymes also confers additional operational properties such as recovery and reusability to the enzyme [8].

One of the most commonly used industrial enzymes is peroxidase [9], an oxidoreductase that can oxidize abroad range of organic compounds. It has several applications in areas such as dye decolorization [10], the production of biofuel cells [11], organic synthesis [12], and bioremediation of phenolic compounds [13]. Other areas of peroxidase application include the agriculture and environmental sectors [1]. Despite these enormous applications, the cost of peroxidase is high and it is not always available, thus the need for the production of peroxidase from fungi, an inexpensive, readily available, and cost-effective source.

The good rate of growth in agro-waste residue and the ability to secrete extracellular enzymes at a high concentration are some of the essential features that make fungi good

sources of enzymes [14,15]. Thus, this study was designed to evaluate the production and immobilization of peroxidase on metallic nanoparticles from a fungal strain cultured by submerging in a fermentation medium fortified with various agro-wastes as the sole carbon source and its ability to decolorize synthetic dyes.

2. Materials and Methods

2.1. Materials

Collection of Soil Sample

Soil samples were collected in a sterile bag from an identified area in Nsukka, Enugu State (6°51′24″ N 7°23′45″ E), Nigeria. Serial dilutions of the samples were prepared up to 10^{-5}. An aliquot was spread on potato dextrose agar (PDA) plates and incubated for 7 days for fungal growth. The isolates obtained were morphologically and taxonomically examined [16]. Isolated fungal strains were maintained on fortified PDA slants and used as stock cultures for the preparation of fresh inoculum for the subsequent experiments.

2.2. Methods

2.2.1. Peroxidase Production

The production of peroxidase was carried out using submerged fermentation in 250 mL flasks containing 100 mL of basal salt medium (BSM) made of peptone (0.3%), KH_2PO_4 (0.06%), $ZnSO_4$ (0.0001%), K_2HPO_4 (0.04%), $FeSO_4$ (0.0005%), $MnSO_4$ (0.05%), $MgSO_4$ (0.05%), and glucose (1%), all in w/v. Prior to inoculation, the media were sterilized by autoclaving and the pH was aseptically adjusted to 6.50, subsequently inoculated with a nine-day-old fungal culture (four loops of mycelium ⌀ 3 mm), and incubated at 30 °C with shaking for nine days. Thereafter, the media were homogenized using an electric homogenizer and the homogenate separated using a centrifuge (Rotina 380 R Benchtop, Tuttlingen, Germany) at 6000 rpm for 60 min at 4 °C. The supernatant was filtered through a four-layer calico cloth and used for the subsequent analysis.

2.2.2. Optimization of Fungal Medium for Peroxidase Production

The conditions for peroxidase production by the organism were studied and optimized using different standard carbon sources (sucrose, xylose, glucose, mannose, lactose, arabinose, and soluble starch) in the fermentation medium at varying concentrations of 0.1–1.0 g/100 mL. The concentration of the best carbon source was varied from 0.5 to 10.0 g/100 mL at intervals of 0.5 g. The medium's pH was also adjusted from pH 3.5 to pH 11.0 at intervals of 0.5 units in order to ascertain the optimal fermentation pH. The optimal incubation temperatures (30–45 °C) were varied at intervals of 5 °C. Furthermore, different agro-wastes such as bambara nut husk, banana peel, orange peel, sugar cane bagasse, and saw dust served as the sole source of carbon in the fermentation medium. After the cultivation, the fermentation broth was homogenized using an electric homogenizer and the homogenate was separated into supernatant and cell debris at 6000 rpm for 60 min at 4 °C using a centrifuge (Rotina 380 R Benchtop, Tuttlingen, Germany). The supernatant was further filtered through a four-layer calico cloth, and the filtrate was utilized to assay for peroxidase's activity.

2.2.3. Time Course Study for Peroxidase Production

The day of the highest peroxidase activity production by the fungal isolate was evaluated by the withdrawal of aliquots from the fermentation broth every day for 15 days.

2.2.4. Peroxidase Purification and Molecular Weight Determination

The crude enzyme was precipitated out of the solution using ammonium sulfate. About 250 g of ammonium sulfate was added in 800 mL of crude enzyme and allowed to stand for 6 h under continuous shaking. The solution was centrifuged at 6000 rpm for 20 min to recover the pellet, and the supernatant was subsequently brought to 70% saturation, which gave the maximum protein precipitation. The pellet recovered from the ammonium

sulfate precipitation was re-suspended in sodium phosphate buffer (pH 8.0; 0.1 M). The precipitated enzyme was introduced onto a (40.5 × 1.4 cm) DEAE-cellulose anion exchanger column equilibrated with 0.1 M sodium phosphate buffer (pH 8.0). The sample was eluted with a discontinuous NaCl gradient of a 0.5, 0.1, 0.15, and 0.2 M concentration of NaCl. The active fractions were subjected to size exclusion chromatography. The active fractions were fractionated by gel filtration on a sephadex G75 column, previously equilibrated with 0.1 M phosphate buffer (pH 8.0). Fractions were collected at a 5 mL flow rate per 5 min, which was used to determine peroxidase's activity and protein concentration. For the determination of the enzyme molecular weight, SDS-PAGE was performed in 12% disc gels, as described by Laemmli [17], and the gels were stained with silver staining as described Switzer et al. [18] under standard conditions.

2.2.5. Enzyme Activity Assay

Peroxidase activity was assayed using the method of Eze [19] by measuring the change in absorbance as it oxidizes the o-dianisidine using a UV/Vis spectrophotometer (6405 Jenway, East Lyme, CT, USA). The assay mixture (3 mL) contained 100 mM phosphate buffer (2 mL, pH 7.0), the substrate (o-dianisidine, 0.3 mL), and the crude enzyme (0.4 mL). The reaction was initiated by the addition of hydrogen peroxide (0.3 mL). The peroxidase's activity was monitored by the change in absorbance (at 470 nm) due to the oxidation of o-dianisidine.

2.2.6. Phylogenetic Analysis of the Fungal Isolate Genome

The isolation of the genomic DNA of the potent fungal isolate was performed as described by Pryce [20]. The amplification of the ITS region was carried out under standard conditions using polymerase chain reaction, where LS266: 5′-GCATTCCCAAACAACTCGA CTC-3′ and V9D: 5′-TTAAGTCCCTGCCCTTTGTA-3′ were used as the universal oligonucleotides for the reverse and forward primers, respectively [20].The generated sequence of nucleotides was used to carry out a blast search in the NCBI database for the retrieval of similar sequences, after which, multiple sequence alignment was accomplished using the ClustalW program, followed by the construction of the phylogenetic tree.

2.2.7. Synthesis and Functionalization of Iron Oxide Magnetic Nanoparticles

The synthesis of iron oxide magnetic nanoparticles (IOMNPs)was carried out as described by Ranjbakhsh et al. [21]. Into a 500 mL round-bottom flask, $FeCl_2 \cdot 4H_2O$ (1.25 g) and $FeCl_3 \cdot 6H_2O$ (3.40 g) were dissolved in de-ionized (100 mL) water at 60 °C. Thereafter, 25% $NH_3 \cdot H_2O$ (6 mL) was added, and the reactant mixture vigorously stirred at 250 rpm for 60 min. The obtained black precipitate was separated from the liquid phase using a magnetic field and washed thrice with phosphate-buffered saline (PBS, 100 mM sodium phosphate, 150 mM NaCl, pH 7.4). In order to functionalize them with the –NH$_2$ groups, IOMNPs (300 mg, dry weight) were incubated with 2% (*v/v*) 3-aminopropyltriethoxysilane (APTS, 30 mL) at 70 °C with shaking (250 rpm) in a water bath. Glutaraldehyde (2%) was added and stirred for 120 min at 350 rpm [22]. After 24 h, they were washed thrice with PBS and maintained in the same buffer at 4 °C until use. The activated IOMNPs were incubated with peroxidase (30 U/mL) at 4 °C for 24 h with continuous shaking at 300 rpm. The IOMNP–peroxidase complex was decanted using a magnet and washed five times with deionized water and stored at 4 °C until further use.

2.2.8. Characterization of IOMNPs

Phase identification of the formulated IOMNPs was performed by X-ray diffraction studies (XRD) (Philips Diffractometer, Amsterdam, The Netherlands). The particle size was determined using dynamic light scattering (DLS)(Malvern Zeta sizer Nano S, Worcestershire, U.K.), and the morphology was determined by scanning electron microscopy (SEM)(FEI Company, Tokyo, Japan). Functional groups were detected using Fourier transform infrared spectroscopy (FTIR)(Shimadzu, Kyoto, Japan). The thermostability of the

nanoparticle was determined using differential scanning calorimetry (DSC)(Shimadzu, Kyoto, Japan) at a heating rate of 10 °C from 60–300 °C in a hermetically sealed aluminum pan.

2.2.9. Effect of Temperature and pH on Free and Immobilized Peroxidase's Activities

The effect of temperature on the free and immobilized peroxidase's activities was determined at different temperatures (30–70 °C). Furthermore, the effect of pH on the free and immobilized peroxidase's activities was carried out at different pH values ranging from 3.5–11.0 using 0.1 M sodium acetate (pH 4.0–5.0), 0.1 M sodium phosphate (pH 6.0–8.0), and 1 M Tris-HCl (pH 9.0). The result is presented as peroxidase residual activity, using the criteria described in the enzyme assay section.

2.2.10. Effect of Free and Immobilized Peroxidase on Substrate Concentration

The rate of two substrates' (guaiacol and pyrogallol) metabolism by peroxidase was carried out at varying concentrations of 0.2–1.2 g/10 mL. The kinetic parameters (K_M, Vmax, $Kcat$, catalytic efficiency) were calculated from the Lineweaver–Burk plotand their derivative constants.

2.2.11. Effect of Organic Solvents on Peroxidase Activity

The influence of some organic solvents—DMSO, methanol, acetone, chloroform, and ethanol—on the free and immobilized peroxidase's activities was evaluated after 60 min of incubation of the enzyme with the organic solvents. The residual activity was measured as described in the enzyme assay section.

2.2.12. Synthetic Dye Decolorization by Free and Immobilized Peroxidase

The ability of the free and immobilized peroxidase to decolorize synthetic dyes was evaluated according to the method of Victor et al. [10]. The dyes used were three (3) azo dyes (Azo Yellow 6, Basic Blue 22, and Azo Brilliant black) and two (2) Vat dyes (Vat Blue 5 and Acid Blue 74). The reaction mixture containing 0.05 M acetate buffer (2.7 mL, pH 5.0), dye solution (0.1 mL), H_2O_2 (0.1 mL), and the free and immobilized peroxidase (0.1 mL each) was incubated at 37 °C for 60 min. Subsequently, the absorbance was read at a wavelength of 614 nm using a JENWAY 6404 UV/VIS spectrophotometer. The percentage of decolorization of each dye was calculated by using the following equation:

$$\text{Percentage decolorization}(\%) = \frac{\text{Ai} - \text{Af}}{\text{Ai}} \times 100 \tag{1}$$

where Ai = initial absorbance before incubation and Af = final absorbance after incubation.

3. Results

Physicochemical conditions (carbon sources, nitrogen sources, pH, temperature, and rate of agitation) were studied for optimal peroxidase production by *Aspergillus flavus* KIGC (Figure 1). The effect of different fermentation temperatures (35–45 °C) was studied to ascertain the optimal fermentation temperature for peroxidase production by *Aspergillus flavus* KIGC. At 35 °C, the highest peroxidase activity (229.12 ± 1.46 U/min) was obtained. Above this temperature, peroxidase production decreased in peroxidase's activity, as shown in Figure 2a. Furthermore, the optimal pH for peroxidase production by the organism was evaluated. The result showed the highest fungal peroxidase production at pH 7.50, with maximum activity of 301.73 U/min (Figure 2b). At the alkaline pH (pH 8.0–11.0), the peroxidase production decreased considerably, ranging from 34.11 to 27.04 U/min.

Carbon is an essential nutrient for microbial growth; hence, different sources of carbon (sucrose, lactose, mannose, glucose, xylose, arabinose, and soluble starch) at varying concentrations (0.1, 0.2, 0.5, 0.8, and 1.0 g/100 mL) were substituted in the fermentation flask for peroxidase production. Peroxidase was produced in the presence of all the carbon sources (sucrose, lactose, mannose, glucose, xylose, arabinose, and soluble starch) at different concentrations. Peroxidase activity was highest 296.40 ± 1.54, 440.17 ± 3.18,

483.96 ± 0.87, 276.63 ± 1.21, and 193.26 ± 0.14 U/min in the fermentation media containing glucose at all concentrations of 0.1, 0.2, 0.5, 0.8, and 1.0 g/100 mL, respectively when compared to other carbon sources (Figure 3a), followed by mannose as the sole carbon source. The least peroxidase's activity (12.05 ± 1.24, 39.30 ± 0.76, 22.86 ± 0.11, 37.87 ± 1.42, and 19.36 ± 0.54 U/min) was obtained from the fermentation flask containing soluble starch at all the concentrations studied. Furthermore, the effect of varying the glucose concentration on the peroxidase's activity was evaluated, and 6 g/L was optimal for peroxidase secretion by *Aspergillus flavus* KIGC (Figure 3b). At 10 g/L of glucose, there was a drastic reduction in peroxidase's activity.
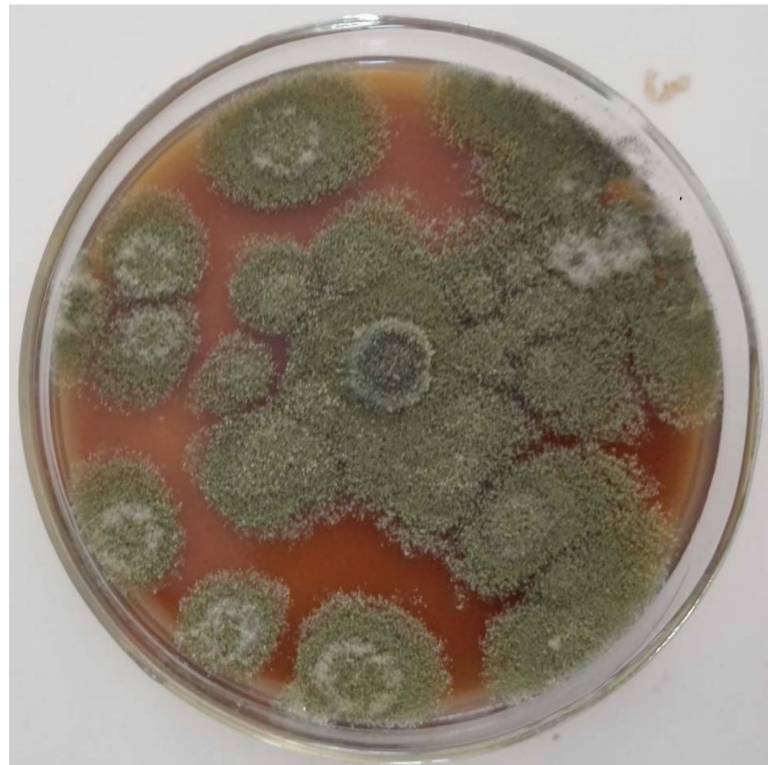

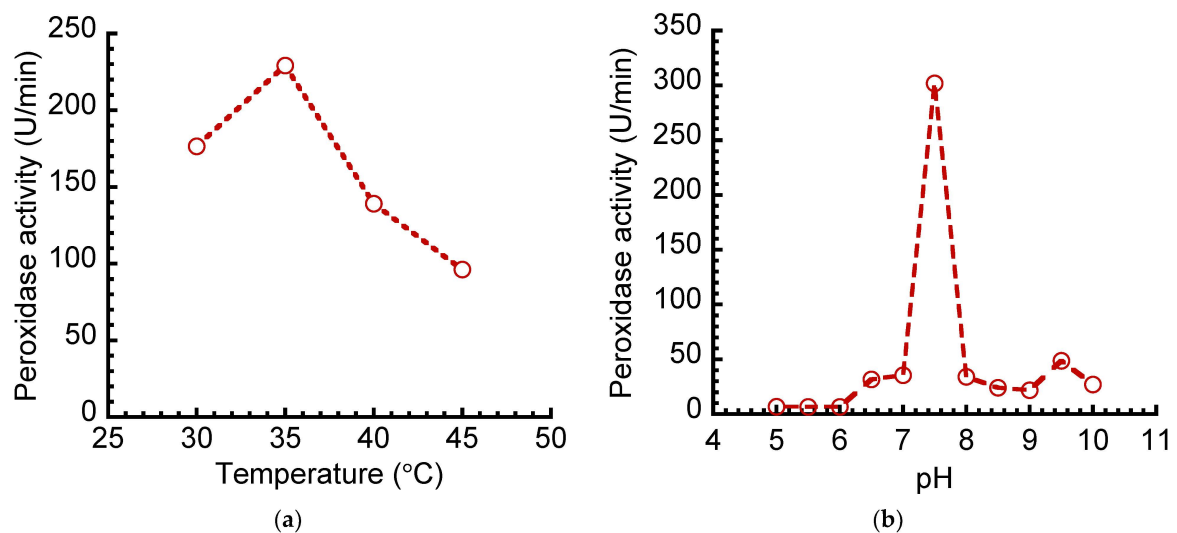**Figure 1.** Pure culture of the *Aspergillus flavus* KIGC.

(a) (b)

Figure 2. Effects of fermentation (**a**) temperature, and (**b**) pH on peroxidase production.
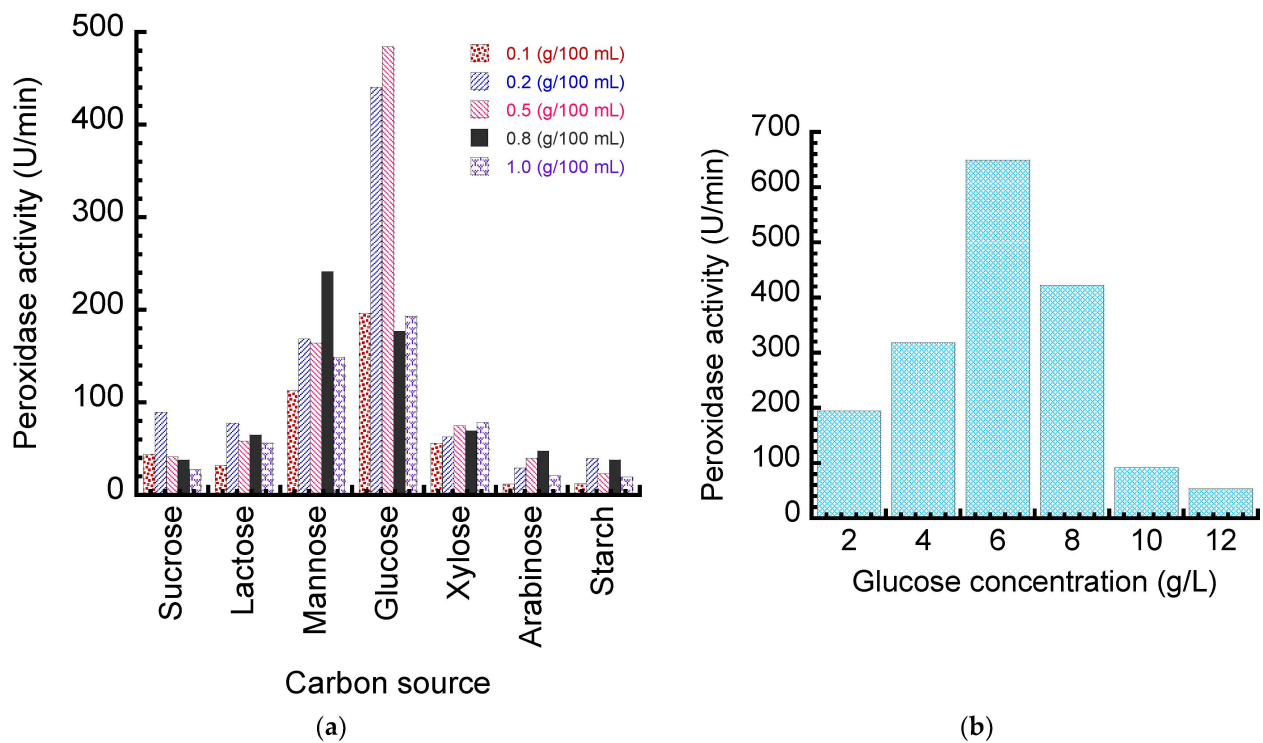
Figure 3. Effects of (**a**) carbon sources and (**b**) glucose concentrations on peroxidase production.

Figure 4 shows the time course study on the production of peroxidase by *Aspergillus flavus* KIGC upon incubation for 15 days. Peroxidase activity was assayed every 24 h, with a progressive increase in peroxidase's activity as the days of fermentation increased. On Day 11, the highest peroxidase activity (946.17 ± 3.25 U/min) was recorded; beyond this day, a concomitant decline in the enzyme activity was obtained.
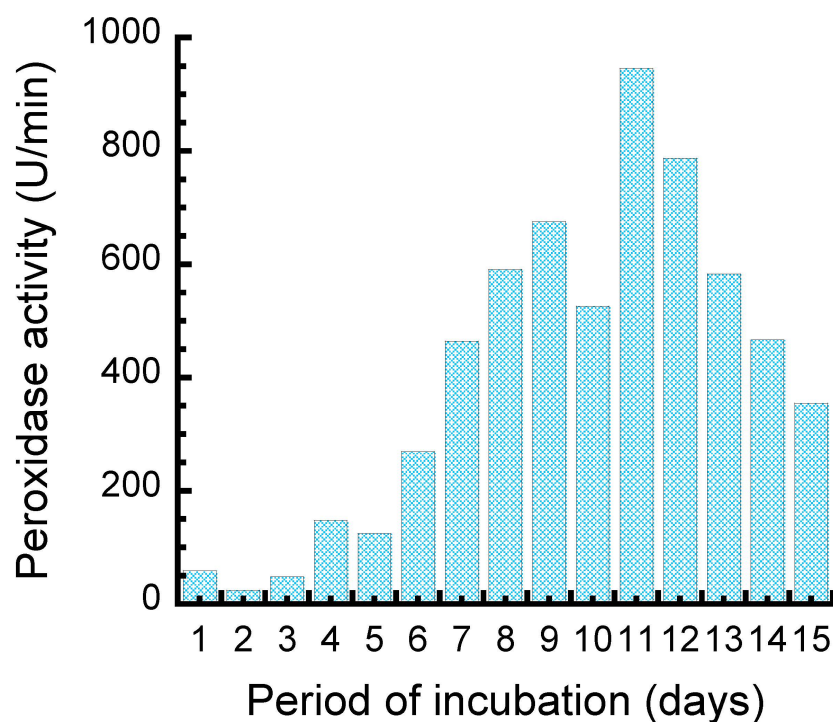

Figure 4. Time course for peroxidase production.

For the cost-effective production of peroxidase from *Aspergillus flavus* KIGC, agro-wastes (bambara husk, orange peel, banana peel, sugarcane bagasse, and sawdust) were used as sources of carbon in the fermentation media. The highest peroxidase production (353.27 ± 0.33 U/min) was obtained in the fermentation medium containing banana peels as the sole carbon source (Figure 5). The fermentation medium with the other carbon sources, orange peels, bambara husk, sugarcane bagasse, and sawdust, had peroxidase's activities of 198.39 ± 1.19, 156.87 ± 0.97, 97.02 ± 0.89, and 0.00 U/min, respectively. There was no fungal growth in the fermentation medium containing sawdust.
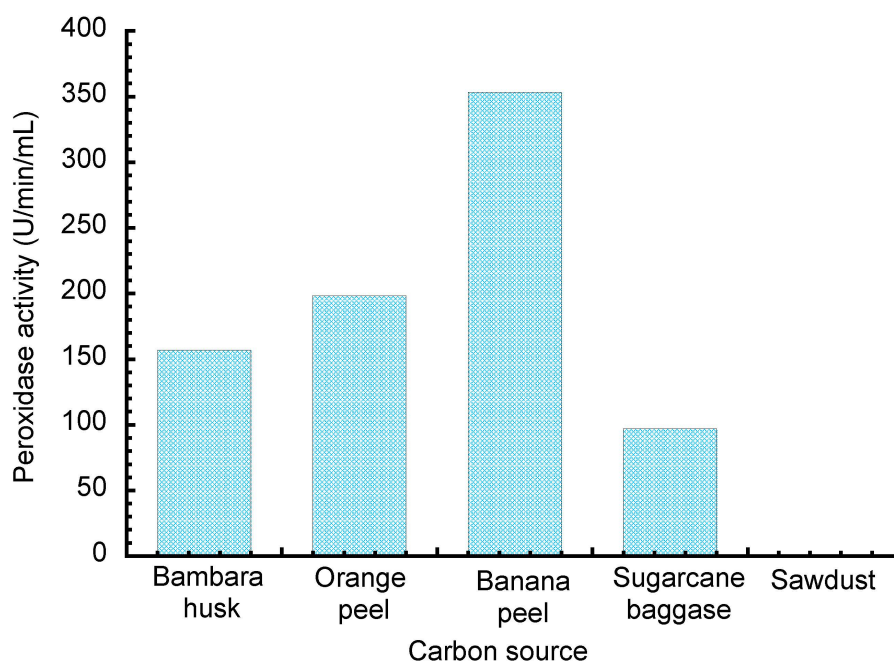

Figure 5. Effects of different agro-wastes as carbon sources on peroxidase production.

Enzyme purification procedures were performed using ammonium sulfate precipitation followed by ion exchange chromatography. The last purification process was gel filtration, giving a final percent yield of 49.72 and a purification fold of 8.86 (Table 1). The molecular weight of the purified enzyme was determined using SDS-PAGE, giving a single band of about 57 KDa (Figure 6).

Table 1. Purification Table for *Aspergillus flavus* KIGC peroxidase.

	Total Protein (mg)	Total Activity (U/min)	Specific Activity (U/min) %	Yield	Purif. Fold
Crude	482.81	7643	57.25	100	1.00
Ammonium sulphate	173.94	20569	118.25	74.40	2.06
Ion exchange	97.13	16599	170.89	60.04	2.98
Gel filtration	27.08	13746	507.60	49.72	8.86

Identity of the Potent Fungal Isolate

The identification of the potent fungal isolate for peroxidase production gave about 99% sequence similarity with *Aspergillus flavus* TN971D17 (Accession Number MH329791) based on ITS region sequencing and phylogenetic analysis and was identified as *Aspergillus flavus* KIGC. The sequence of nucleotides was submitted to the NCBI GenBank with Accession Number MT951631.The clustering of *A. flavus* KIGC and other related sequences is shown in Figure 7.
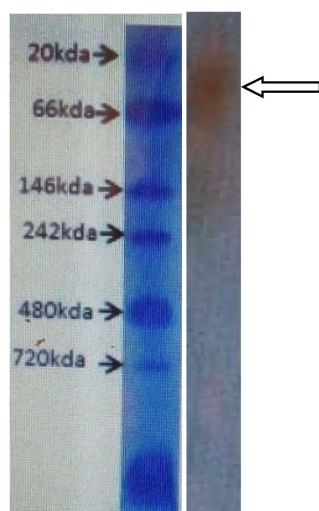
Figure 6. SDS-PAGE analysis of purified peroxidase.
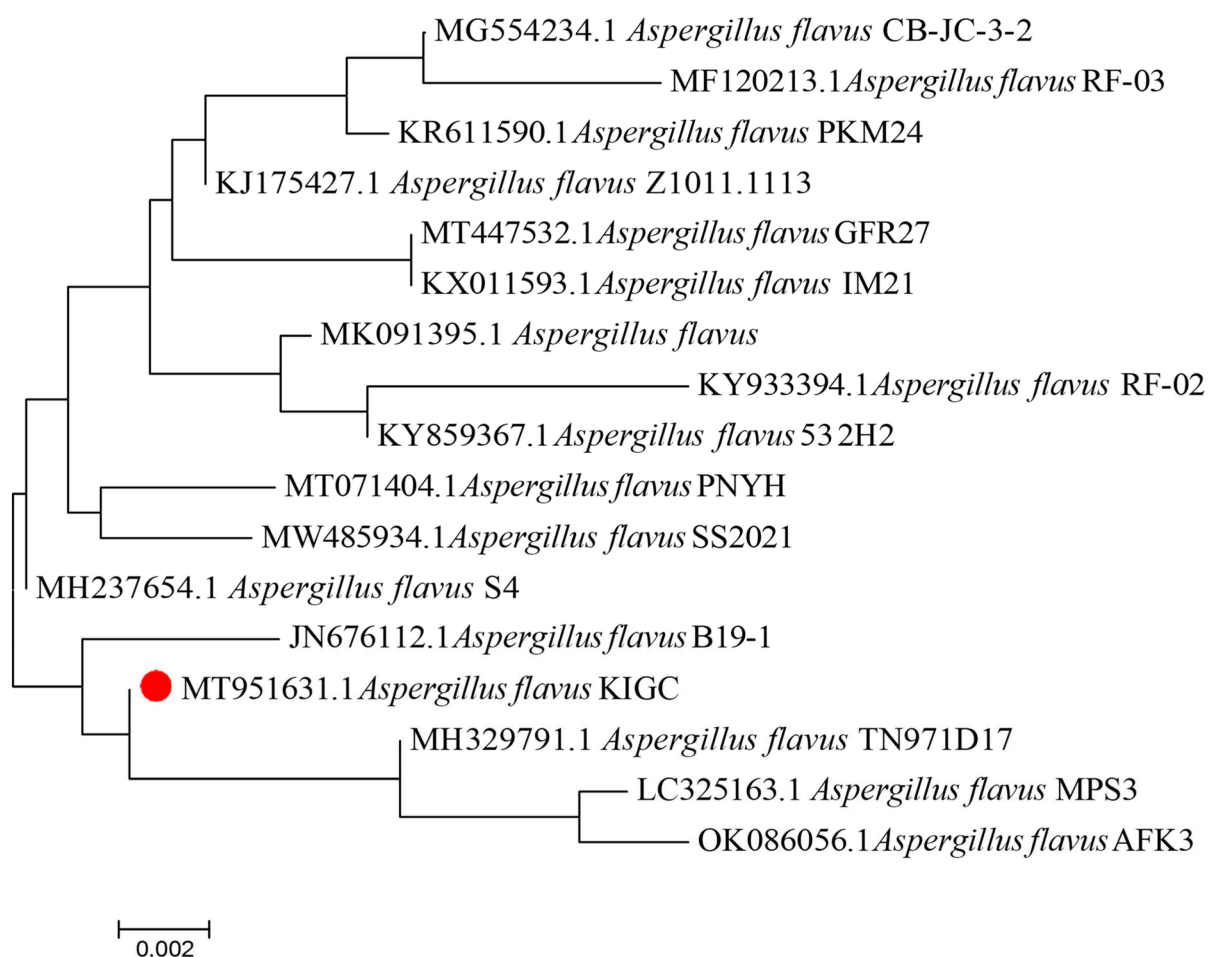
Figure 7. A phylogenetic tree showing the fungal isolate–*Aspergillus flavus* KIGC under investigation (indicated with red symbol) and other reference sequences retrieved from the NCBI GenBank.

The immobilization of peroxidase on metallic nanoparticles was carried out using glutaraldehyde as the cross-linker between surface basic amino acids and glutaraldehyde groups on the surface of the particle [22] (Patel et al., 2018). The particle sizes of the free synthesized metallic nanoparticle and metallic-nanoparticle-immobilized-peroxidase

were 76.20, 48.01, and 481.20 nm, respectively (Figure 8). The thermostability of the free synthesized metallic and immobilized enzyme was also studied using differential scanning calorimetry (DSC). The DSC thermogram of the formulated nanoparticle showed a melting endothermic peak of 193.97 °C (Figure 9). After peroxidase immobilization onto the metallic nanoparticle, the thermogram showed a melting endothermic peak of 110.92 °C with a broad peak.
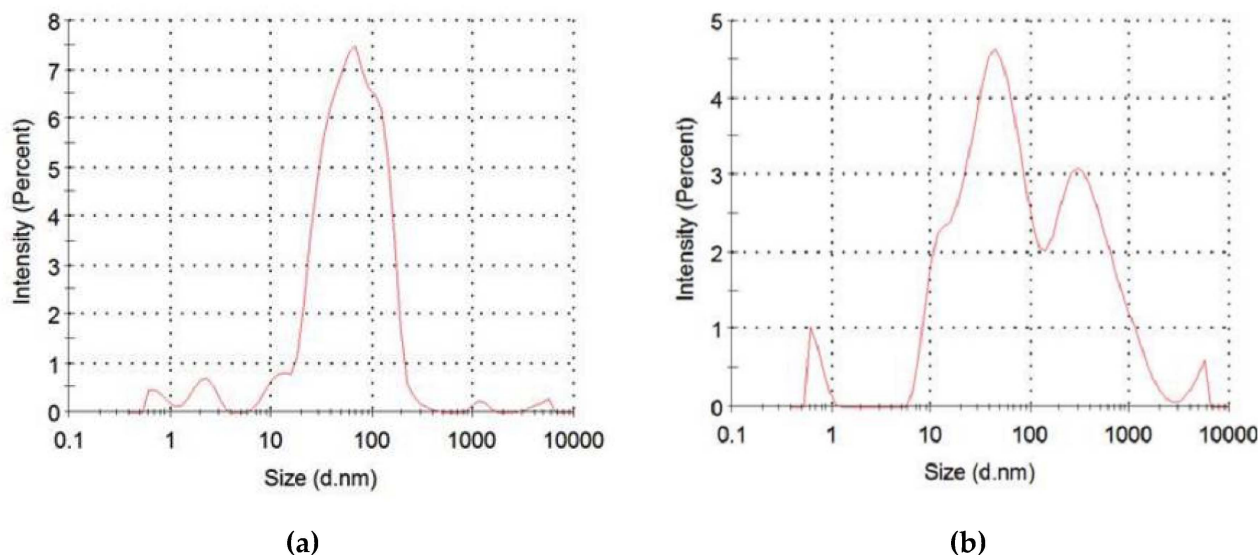

(a)   **(b)**

Figure 8. Intensity size distribution of the synthesized iron oxide magnetic nanoparticles and the IOMNP-immobilized peroxidase. (**a**) IOMNP; (**b**) IOMNP-immobilized peroxidase.
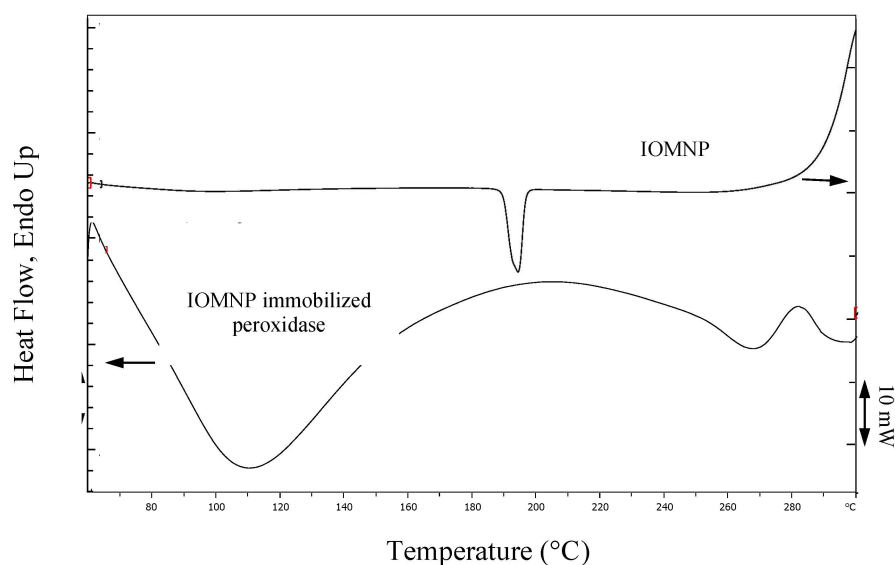
Figure 9. DSC thermogram of the synthesized iron oxide magnetic nanoparticles and the IOMNP-immobilized peroxidase.

Spectra of the nanoparticles and the nanoparticle-immobilized peroxidase were evaluated using FTIR (Figure 10). Two prominent bands were observed in the synthesized IOMNPs at 3000–3400 cm^{-1} and 1625 cm^{-1}. Upon functionalization of the IOMNPs with ATPS and subsequent anchoring of the enzyme through the glutaraldehyde spacer arm, the broad 3000–3400 cm^{-1} transformed into three peaks within the band region.

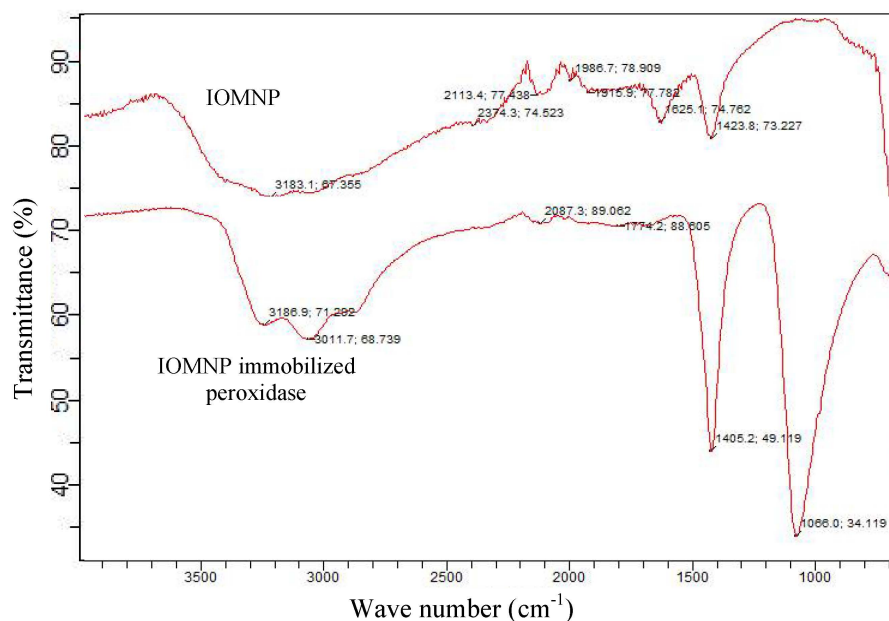**Figure 10.** FTIR spectra of the synthesized iron oxide magnetic nanoparticles and the IOMNP-immobilized peroxidase.

The XRD patterns of the free magnetic nanoparticles and magnetic-nanoparticle-immobilized peroxidase are shown in Figure 11. There were no sharp diffraction peaks in the metallic-nanoparticle-immobilized-peroxidase, unlike the free synthesized metallic nanoparticle. Furthermore, the morphology of the synthesized nanoparticles and nanoparticle-immobilized-peroxidase was studied using scanning electron microscopy (Figure 12). Aggregates of the nanoparticles were seen clustered together with smooth surfaces in the synthesized IOMNPs (Figure 12a). After the functionalization of the enzyme through the glutaraldehyde spacer arm, the surfaces of the composite became less smooth and indistinct, with a greater proportion of open pockets/domains (Figure 12b).
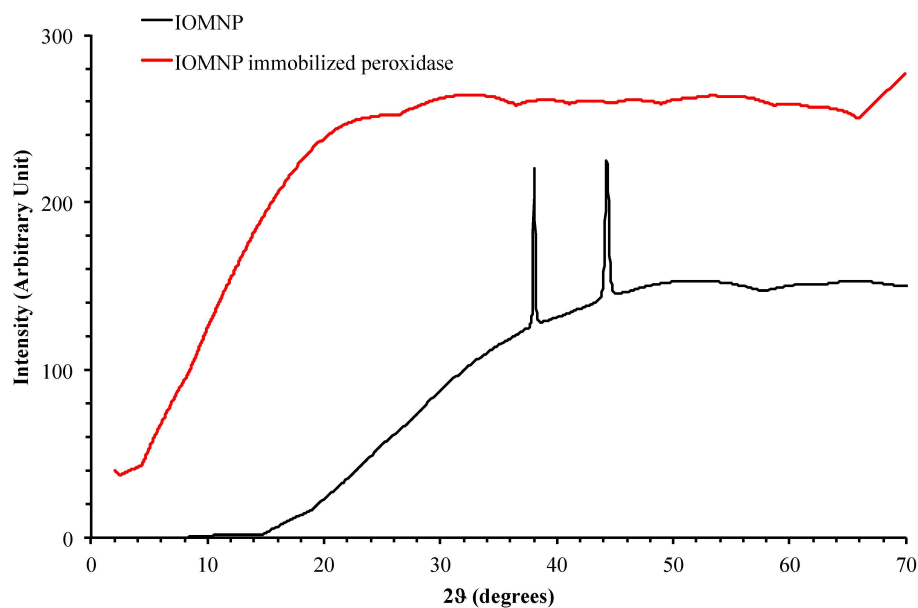

Figure 11. XRD patterns of the synthesized iron oxide magnetic nanoparticles and the IOMNP-immobilized peroxidase.
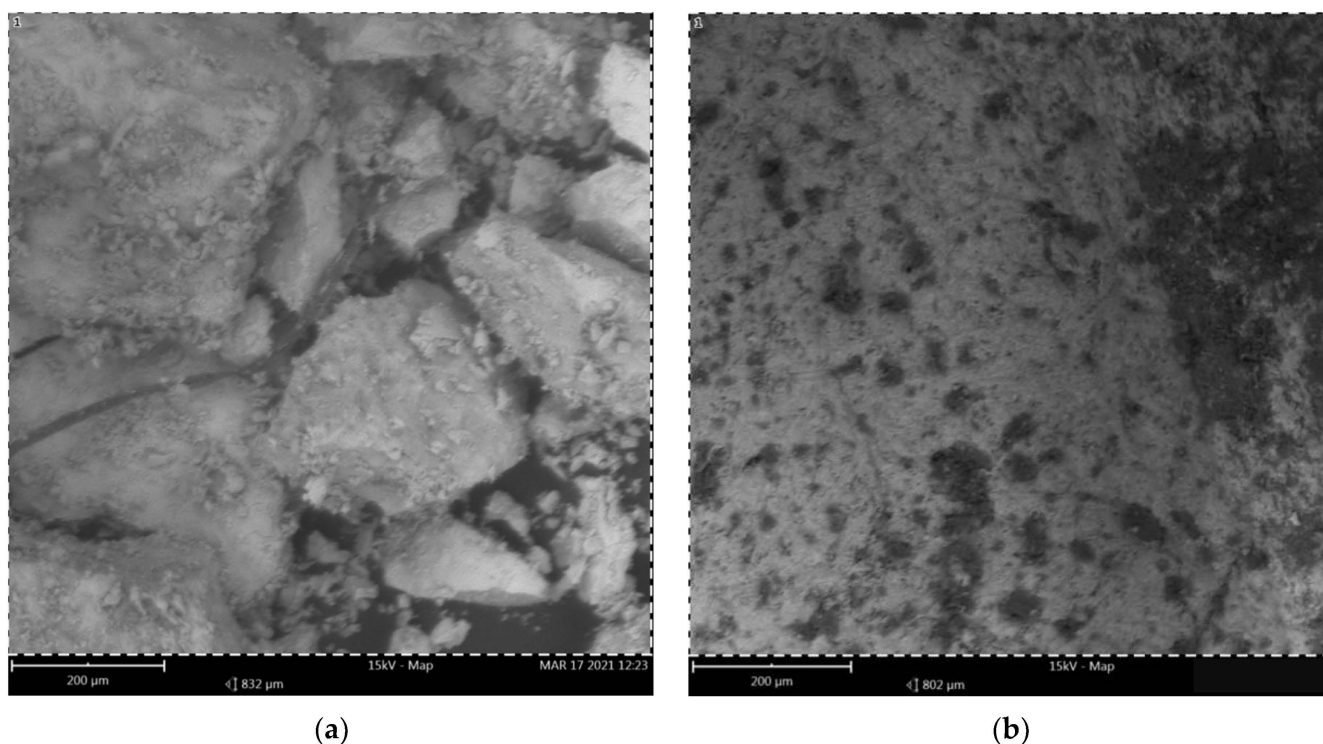
(**a**)   (**b**)

Figure 12. SEM images of the synthesized iron oxide magnetic nanoparticles (**a**) and the IOMNP-immobilized peroxidase (**b**).

The results of the optimal temperature and pH study of the free and immobilized peroxidase's activity are shown in Figure 13a. The optimal temperatures were 75 and 70 °C, respectively, for the free and immobilized peroxidase's activities. There was a successive increase in the enzyme activity as the temperature increased until the optimum temperatures, after which a drastic decrease in the enzyme activity was recorded; however, the immobilized peroxidase had higher activity (826.08 ± 0.32 U/min) than the free enzyme (556.61 ± 1.73 U/min). Similarly, both the free and immobilized peroxidase showed activities in the slightly acidic pH region and at pH 9.0, respectively. There were two high peroxidase peaks for the free enzyme at pH 5 (511.30 ± 0.52 U/min) and pH 9.0 (443.96 ± 0.34 U/min). At both pH 6.5 and 9.0, the peroxidase's activities were high for the immobilized enzyme (Figure 13b); as the pH tended towards basicity, there was a decline in the peroxidase's activity, and the least activity was obtained at pH 9.5.

To study the kinetic parameters of both the free and immobilized peroxidase, varying concentrations of guaiacol and pyrogallol were used at a fixed concentration of H_2O_2. The kinetics parameters for the free peroxidase (K_M) for guaiacol and pyrogallol were 0.135 and 0.243 mM and a V_{max} of 357.14 and 333.33 µmol/min, respectively. Similarly, 0.075 and 1.886 mM were the K_M values obtained for the immobilized peroxidase, while 238.09 and 1000 µmoL/min were the V_{max} of the immobilized peroxidase, respectively (Table 2). Furthermore, 90.66 and 75.55 moL/S^{-1} were the catalytic efficiencies (turnover rate of guaiacol molecules) of the immobilized and free enzyme, while 39.17 and 15.94 were the catalytic efficiencies for the free and immobilized enzyme on pyrogallol as the substrate, respectively.

The influence of varying concentrations (20, 40, 60, and 80%) of some commonly used organic solvents (DMSO, methanol, acetone, chloroform, and ethanol) on the free and immobilized peroxidase's activity after 60 min incubation was evaluated. At a 20% concentration of all the solvents, more than 80% of the peroxidase's activity was retained in both the free and immobilized peroxidase (Figure 14). For the free enzyme, there was a drastic reduction in the peroxidase's activity as the concentration of DMSO and acetone increased to 80%, resulting in residual activities of 44.73 ± 0.69 and 50.11 ± 1.69 U/min,

respectively (Figure 14a). More than 70% residual activity of the peroxidase was recorded after incubation of the enzyme with methanol and ethanol at all concentrations. Notably, the residual activity of the peroxidase increased considerably after incubating the immobilized enzyme for 60 min. At an 80% concentration, more than 60% of the peroxidase's activity was recovered among all organic solvents except for chloroform, which gave 47.72 ± 0.18%. The peroxidase immobilized on the iron oxide magnetic nanoparticles exhibited high tolerance when incubated with ethanol > acetone > DMSO > methanol > chloroform, suggesting that ethanol is a better solvent (Figure 14b).
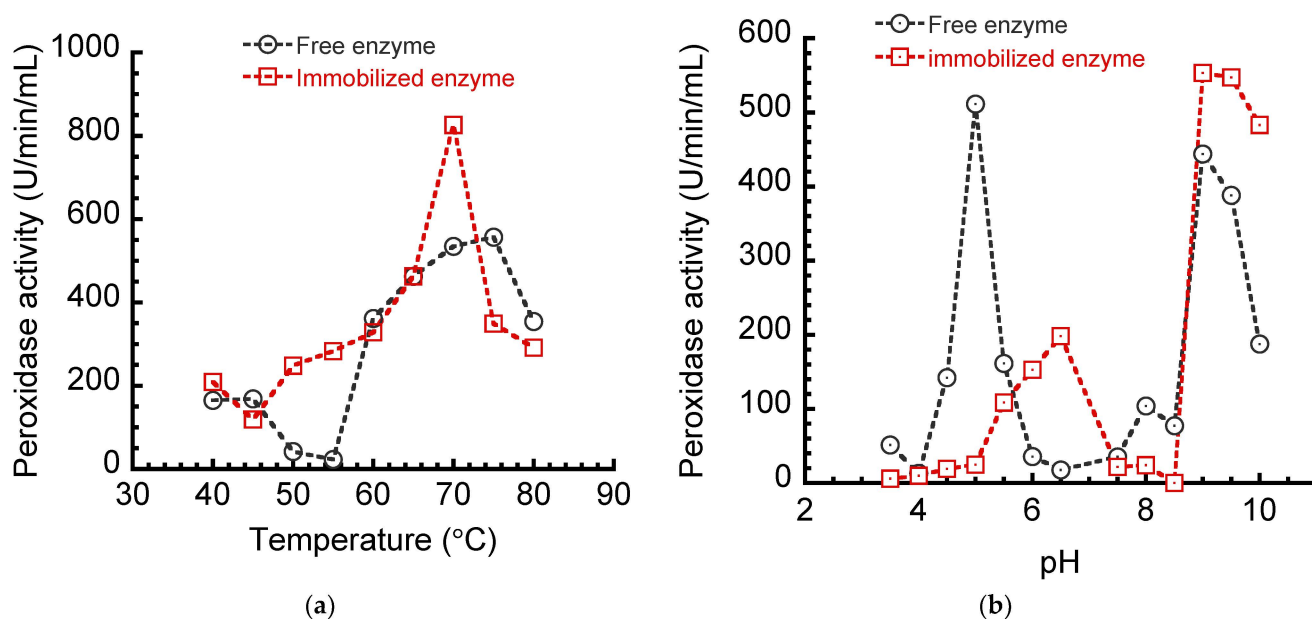

(**a**)   (**b**)

Figure 13. Effects of (**a**) temperature and (**b**) pH on the activity of free and immobilized fungal peroxidase.

Table 2. Kinetics parameters of free and immobilizedperoxidase.

Free Enzyme Immobilized Enzyme	Guaiacol	Pyrogallol	Guaiacol	Pyrogallol
Km (mM)	0.135	0.243	0.075	1.886
Vmax (μmol/min)	357.14	333.33	238.09	1000
$\frac{Vmax}{Km}$	2645.25	1371.74	3174.53	530.22
Kcat (Min^{-1})	10.204	9.52	6.80	28.57
Catalytic Efficiency (Mol/S^{-1})	75.55	39.17	90.66	15.19

The ability of free and immobilized peroxidase to decolorize Azo Yellow 6, Basic Blue 22, Azo Brilliant black, Vat Blue 5, and Acid Blue 74 was evaluated after an incubation time of 120 min (Figure 15). The free enzyme showed different decolorization rates of textile dyes after 120 min including Azo yellow 6 (76 ± 0.33%), Blue basic 22 (68 ± 2.43%), Azo brilliant Black (55 ± 1.37%), Vat Blue 5 (69 ± 1.35%), and Acid Blue 74 (64 ± 0.75%). On the other hand, the immobilized enzyme also exhibited different rates of textile dye decolorization after 120 min as Azo yellow 6 (89 ± 1.77%), Blue basic 22 (90 ± 0.82%), Azo brilliant Black (71 ± 0.77%), Vat Blue 5 (86 ± 1.60%), and Acid Blue 74 (75 ± 2.08%).
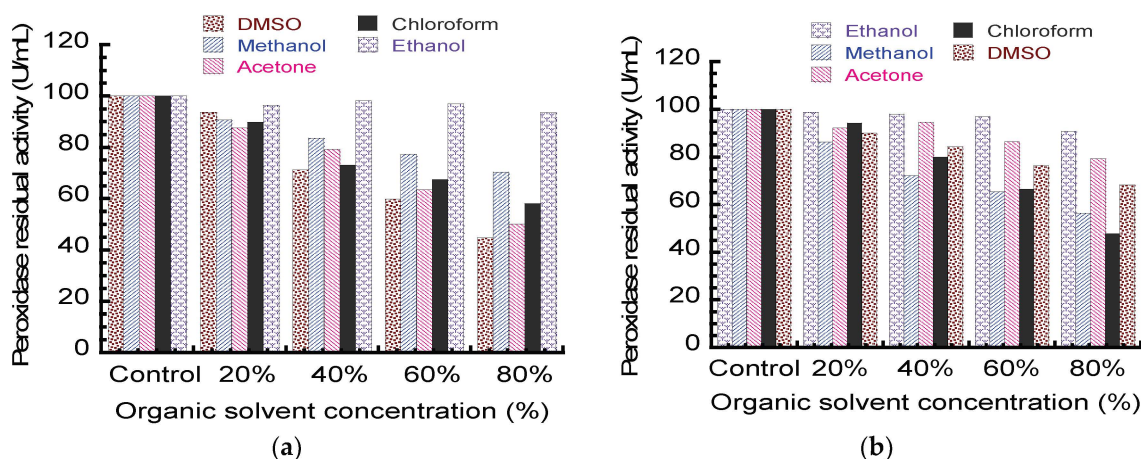
Figure 14. Effect of organic solvents on the (**a**) free and (**b**) iron oxide-magnetic-nanoparticle-immobilized peroxidase's activity.
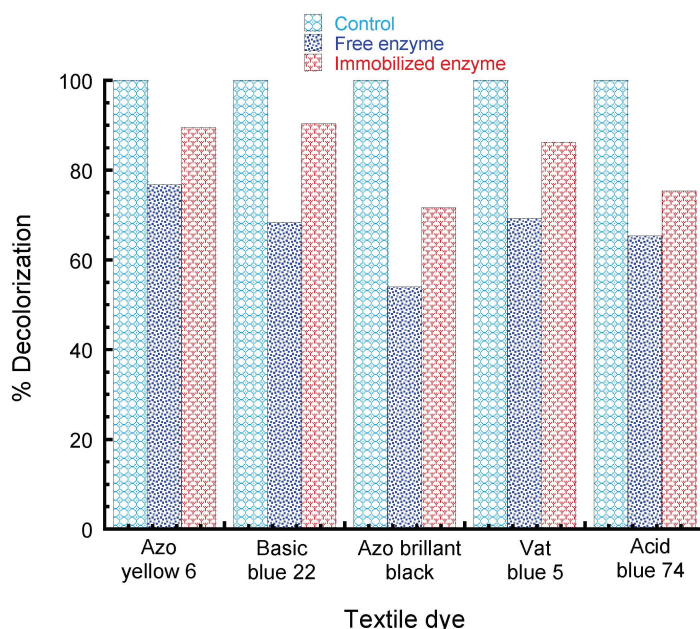

Figure 15. Decolorization potentials of the free and immobilized peroxidase on textile dyes.

4. Discussion

Aspergillus species are important sources of enzymes such as laccase [15], pectinase [23], peroxidase [24], and amylases [25]. The extracellular secretion of peroxidase by the isolate was confirmed by the brown coloration of the solid media as a result of guaiacol oxidation. One of the major factors that affects biomolecule production is the constituent of the medium [26]. Thus, inexpensive and readily available agro-wastes were used as alternative sources of carbon in the fermentation medium. The medium containing banana peel showed a high yield of peroxidase; this could be attributed to the presence of some essential nutrients in the peel that encourage microbial growth. The day of the highest peroxidase activity was recorded on Day 11 of fermentation. Previously, different agro wastes have been reported as good sources of carbon for microbes. Prajapati et al. [24] employed citrus peel in the production of microbial enzymes. Similarly, orange peel and pulp residues were used in enzyme production by some microbial strains [27,28]. Asgher et al. [29] reported the use of corncob in the production of peroxidase by *T. versicolor* on Day 5. Furthermore, enzyme production by *P. ostreatus* and *T. hirsuta* was highest on Day 9

of fermentation [30,31]. These differences in the day of highest peroxidase activity could be due to variations in the species, the source of organism isolation, and the nutrient composition of the medium. Day 9 was reported as the day of the highest enzyme production by Omeje et al. [15].

The final purification fold of the enzyme following sequential ammonium sulfate, ion exchange, and gel filtration procedures was 8.86 (Table 1). Khatri et al. [32] purified enzyme 1.2-fold from *Aspergillus niger* with a specific activity of 8.33 U/min/mg. Furthermore, Dange and Harke [33] purified enzyme from *A. oryzae* up to 67.20%, while 30.65% of activity was reported by Omeje et al. [15] in their work on fungal enzyme. After several steps of enzyme purification (Table 1), a molecular mass of 57 KDa was recorded using SDS-PAGE (Figure 6). Researchers have reported similar findings. A molecular mass of 56KDa was reported for *C. cardunculus* peroxidase [34]. The fungal isolate presumably identified as the KIGC strain was confirmed as *Aspergillus flavus* due to the similarity of the sequence with other sequences in the NCBI database and the nucleotide sequence deposited in GenBank (MT951631). *Aspergillus* spp. have found numerous applications in biotechnological and industrial processes as potential sources for the production of versatile metabolites [35].

The intensity size distribution of the IOMNPs gave a modal diameter of 76.20 nm, and upon immobilization of the enzyme, a new peak diameter of 481.20 nm appeared due to the anchoring of the enzyme onto the nanoparticles (Figure 8). The enzyme-immobilized iron oxide metallic nanoparticles showed a broad melting peak temperature of 110.92 °C, from 193.97 °C recorded for the bare nanoparticles. The melting temperature of the composite is quite high and would be suitable for most industrial applications operating below 110 °C. The broadness of the endothermic peak at 110.92 °C could be due to water molecules adsorbed unto the surface of the composite material (Figure 9). Two prominent bands observed at 3000–3400 cm^{-1} and 1625 cm^{-1} for the synthesized IOMNPs correspond to OH-stretching and OH-bending, respectively, of the metallic NPs. The immobilization of the enzyme onto the IOMNPs through ATPS and the glutaraldehyde spacer arm transformed the broad 3000–3400 cm^{-1} bands into three peaks, corresponding to the vibrations of secondary amines, N-Hof the enzyme's amino groups, and those of the APTS, suggesting firm anchoring of the enzyme onto the IOMNPs. Furthermore, the peak at 1625 cm^{-1} of the bare IOMNPs disappeared upon immobilization of the enzyme onto the NPs, resulting ina less-prominent peak at 1774 cm^{-1}, due to the C=O stretching of glutaraldehyde (Figure 10). Similarly, the disappearance of the diffraction peaks on the free IOMNPs upon enzyme immobilization suggests that the formulated enzyme–NP composite material possesses no crystalline phases as a result of the immobilization of the enzyme, unlike the two prominent peaks on the bare IOMNPs due to the lattice arrangement of the iron atoms (Figure 11). From the SEM results, the anchoring of the enzyme onto the metallic nanoparticles considerably increased the roughness of the surface of the enzyme–NP composite with the appearance of open domains therein (Figure 12). These observations are indicative of the change in morphology and the increase in the average size of the IOMNPs upon enzyme immobilization.

The temperature and pH are some important factors that affect enzyme activity. The optimal temperatures for both free and immobilized peroxidase were 75 and 70 °C, respectively (Figure 13a). These are high when compared to the temperature optima of 40 °C reported by [9]. Furthermore, 45 °C was the optimal temperature of peroxidase extracted from cabbage [10]. Similarly, the optimum pH peaks at 5.0 and 9.0 were obtained for the free enzyme, while the metallic-nanoparticle-immobilized peroxidase showed an optimum pH of 6.5 and 9.0, respectively. The appearance of the two peroxidase activity peaks at both acidic and alkaline pH for both the free and immobilized peroxidase could be attributed to the presence of enzyme isoforms, which aid the survival of the enzymes at different pH ranges. Reference [15] reported an optimum pH of 7.5 for fungal enzyme. This result is in accordance with the work by [10], who reported an optimum pH of 5.0. The pH 5.0 obtained for the free enzyme is in accordance with the report by Osuji et al. [36]. The variation in the peroxidase's activity in the acidic region could be associated with the presence

of the immobilized material, which could not interfere with the enzyme activity in the alkaline region (Figure 13b) The kinetic features of the metallic-nanoparticle-immobilized peroxidase on two substrates (guaiacol and pyrogallol), indicated in Table 1, show that the enzyme has high affinity for guaiacol (K_M = 0.075 mM), with a catalytic efficiency of 90.66 M^{-1} s^{-1}, compared to pyrogallol (K_M = 1.886 mM),with a catalytic efficiency (turnover rate) of 15.19 M^{-1} s^{-1}. The free enzyme showed more affinity for guaiacol (K_M = 0.135 mM) than pyrogallol (K_M = 0.243 mM), with a higher catalytic efficiency of 75.55 M^{-1} s^{-1}. A kinetic parameter(K_M) of 2.00 mg/mL has been reportedforguaiacol [9], while [10] reported a Michaelis constant (K_m) of 3.68Mm on O-dianisidine as the substrate. Previous reports have shown that peroxidase has more affinity towards guaiacol than pyrogallol and o-dianisidine [37–39].

Figure 14a shows different residual peroxidase activity after 60 min of incubation of the free peroxidase with some common industrial solvents (DMSO, methanol, acetone, chloroform, and ethanol). At an 80% concentration of ethanol and methanol, more than 70% peroxidase residual activity was recovered. The ability of the enzyme to offer resistance to some organic industrial solvents makes it more versatile for industrial uses [1]; hence, the ability of the purified fungal peroxidase to retain more than 60% of its activity in these solvents (Figure 14b) suggests it as a good industrial enzyme. Furthermore, peroxidase of soybean hull origin has shown the highest activity in ethanol, acetone, and methanol [40]. Similarly, Reference [1] reported the highest peroxidase activity in ethanol and butanol, and the report by [41] showed 40% peroxidase activity in the presence of ethanol.

The dye decolorization potentials of free and metallic-nanoparticle-immobilized peroxidase of Azo yellow 6, Basic blue 22, Azo brilliant black, Vat blue 5, and Acid blue 74 were compared with the free enzyme. The metallic-nanoparticle-immobilized peroxidase showed more decolorization ability on all the dyes studied as compared to that of the free enzyme (Figure 15). Reference [10] earlier reported the synthetic dye decolorization potential of peroxidase. Furthermore, Reference [15] reported the decolorization of dyes by fungal enzyme. The decolorization of crystal violet using free peroxidase was reported by [42] and of bromophenol blue by [43]. Reference [44] reported the high dye decolorization efficiency by immobilized lignin peroxidase.

5. Conclusions

Fungal peroxidase was extracted on the 11th day of submerged fermentation while banana peel served as the sole carbon source, purified, and successfully immobilized onto iron oxide magnetic nanoparticle. The immobilized enzyme showed a high optimal temperature and was active within a broad range of pH, with better kinetic results of affinity and catalytic efficiency (turnover rate) towards guaiacol as the substrate. Furthermore, it possessed greater dye decolorization potential than the free enzyme and was tolerant to some organic solvents, which makes it an important biocatalyst for various industrial applications.

Author Contributions: Conceptualization, K.O.O., B.O.E. and S.O.O.E.; methodology, K.O.O., B.O.E. and J.N.O.; software, K.O.O. and E.C.O.; validation, K.O.O., B.O.E. and S.O.O.E.; formal analysis, K.O.O., B.O.E. and S.O.O.E.; investigation, K.O.O., C.M., B.O.E., E.C.O., J.N.O. and S.O.O.E.; resources, K.O.O., C.M., B.O.E., E.C.O., J.N.O.; data curation, K.O.O., C.M., B.O.E., E.C.O., J.N.O., N.E.N. and S.O.O.E.; writing—original draft preparation, K.O.O., B.O.E., N.E.N. and S.O.O.E.; writing-review and editing, K.O.O., B.O.E., E.C.O. and S.O.O.E.; visualization, K.O.O., C.M., B.O.E., E.C.O., N.E.N.; supervision, K.O.O. and S.O.O.E.; project administration, K.O.O., C.M. and S.O.O.E. All authors have read and agreed to the published version of the manuscript.

Conflicts of Interest: The authors declare no conflict of interest.

References

1. Pandey, V.P.; Rani, J.; Jaiswal, N.; Singh, S.; Awasthi, M.; Shasany, A.K.; Tiwari, S.; Dwivedi, U. Chitosan immobilized novel peroxidase from Azadirachta indica: Characterization and application. *Int. J. Biol. Macromol.* **2017**, *104*, 1713–1720. [CrossRef] [PubMed]
2. Patel, S.K.S.; Choi, S.H.; Kang, Y.C.; Lee, J.K. Eco-friendly composite of Fe_3O_4-reduced graphene oxide particles for efficient enzyme immobilization. *ACS Appl. Mater. Interfaces* **2017**, *9*, 2213–2222. [CrossRef] [PubMed]
3. Patel, S.K.S.; Otari, S.V.; Li, J.; Kim, D.R.; Kim, S.C.; Cho, B.K.; Kalia, V.C.; Kang, Y.C.; Lee, J.K. Synthesis of cross-linked protein-metal hybrid nanoflowers and its application in repeated batch decolorization of synthetic dyes. *J. Hazard. Mater.* **2020**, *347*, 442–450. [CrossRef] [PubMed]
4. Cui, J.D.; Cui, L.L.; Zhang, S.P.; Zhang, Y.F.; Su, Z.G.; Ma, G.H. Hybrid magnetic cross-linked enzyme aggregates of phenylalanine ammonia lyase from rhodotorula glutinis. *PLoS ONE* **2014**, *9*, e97221. [CrossRef] [PubMed]
5. de Sousa, M.; Silva, G.B.; Pessela, B.C.; Gonçalves, L.R.B. Preparation of CLEAs and magnetic CLEAs of a recombinant L-arabinose isomerase for D-tagatose synthesis. *Enzyme Microb. Technol.* **2020**, *138*, 109566. [CrossRef] [PubMed]
6. Vaghari, H.; Jafarizadeh-Malmiri, H.; Mohammadlou, M.; Berenjian, A.; Anarjan, N.; Jafari, N.; Nasiri, S. Application of magnetic nanoparticles in smart enzyme immobilization. *Biotechnol. Lett.* **2016**, *38*, 223–233. [CrossRef] [PubMed]
7. Otari, S.V.; Patel, S.K.S.; Kim, S.Y.; Haw, J.R.; Kalia, V.C.; Kim, I.W.; Lee, J.K. Copper Ferrite Magnetic Nanoparticles for the Immobilization of Enzyme. *Indian J. Microbiol.* **2019**, *59*, 105–108. [CrossRef] [PubMed]
8. Singh, R.K.; Tiwari, M.K.; Singh, R.; Lee, J.K. From protein engineering to immobilization: Promising strategies for the upgrade of industrial enzymes. *Int. J. Mol. Sci.* **2013**, *14*, 1232–1277. [CrossRef]
9. Omeje, K.O.; Eze, S.O.O. Properties of partially purified peroxidase extracted from the fruit of *Solanum* spp grown in Enugu north (Variety A) and Plateau central (variety B) zones of Nigeria. *Biokemistri* **2018**, *30*, 1–12.
10. Victor, C.C.; Omeje, K.O.; Eze, S.O.O.; Ezugwu, A.L.; Chilaka, F.C.; Onwurah, I.N.E.; Ukoha, P.O. Decolorization of synthetic dyes using partially purified peroxidase from green cabbage (Brassica oleracea). *Songklanakarin J. Sci. Technol.* **2019**, *41*, 783–787.
11. Chung, Y.; Tannia, D.C.; Kwon, Y. Glucose biofuel cells using bi-enzyme catalysts including glucose oxidase, horseradish peroxidase and terephthalaldehyde crosslinker. *Chem. Eng. J.* **2018**, *334*, 1085–1092. [CrossRef]
12. Lopes, G.R.; Pinto, D.C.G.A.; Silva, A.M.S. Horseradish peroxidase (HRP) as a tool in green chemistry. *RSC Adv.* **2014**, *4*, 37244–37265. [CrossRef]
13. Zhang, F.; Zhang, W.; Zhao, L.F.; Liu, H. Degradation of phenol with horseradish peroxidase immobilized on ZnO nanocrystals under combined irradiation of microwaves and ultrasound. *Desalin. Water Treat.* **2016**, *57*, 24406–24416. [CrossRef]
14. Balaji, V.; Arulazhagan, P.; Ebenezer, P. Enzymatic bioremediation of polyaromatic hydrocarbons by fungal consortia enriched from petroleum contaminated soil and oil seeds. *J. Environ. Biol.* **2014**, *35*, 521–529.
15. Omeje, K.O.; Nnolim, N.E.; Ezema, B.O.; Ozioko, J.N.; Eze, S.O.O. Synthetic dyes decolorization potential of agroindustrial waste-derived thermo-active laccase from Aspergillus species. *Biocatal. Agric. Biotechnol.* **2020**, *29*, 101800. [CrossRef]
16. Gilman, J.C.A. *Manual of Soil Fungi*, 2nd ed.; Iowa State College Press: Ames, IA, USA, 1971; pp. 448–456.
17. Laemmli, U.K. Cleavage of structural proteins during the assembly of the head of bacteriophage T4. *Nature* **1970**, *227*, 680–685. [CrossRef]
18. Switzer, R.C.; Merril, C.R.; Shifrin, S. A highly sensitive silver stain for detecting proteins and peptides in polyacrylamide gels. *Anal. Biochem.* **1979**, *98*, 231–237. [CrossRef]
19. Eze, S.O.O. Kinetic analysis of the thermostability of peroxidase from African oil bean (Pentaclethra macrophylla Benth) seeds. *J. Biochem. Technol.* **2012**, *4*, 459–463.
20. Pryce, T.M.; Palladino, S.; Kay, I.D.; Coombs, G.W. Erratum: Rapid identification of fungi by sequencing the ITS1 and ITS2 regions using an automated capillary electrophoresis system (Medical Mycology (2003) 41 (369-381)). *Med. Mycol.* **2004**, *42*, 93.
21. Ranjbakhsh, E.; Bordbar, A.K.; Abbasi, M.; Khosropour, A.R.; Shams, E. Enhancement of stability and catalytic activity of immobilized lipase on silica-coated modified magnetite nanoparticles. *Chem. Eng. J.* **2012**, *179*, 272–276. [CrossRef]
22. Cruz-Izquierdo, Á.; Picó, E.A.; López, C.; Serra, J.L.; Llama, M.J. Magnetic Cross-Linked Enzyme Aggregates (mCLEAs) of Candida antarctica lipase: An efficient and stable biocatalyst for biodiesel synthesis. *PLoS ONE* **2014**, *9*, e115202. [CrossRef]
23. Rehman, H.U.; Nawaz, M.A.; Aman, A.; Baloch, A.H.; Qader, S.A.U. Immobilization of pectinase from Bacillus licheniformis KIBGE-IB21 on chitosan beads for continuous degradation of pectin polymers. *Biocatal. Agric. Biotechnol.* **2014**, *3*, 282–287. [CrossRef]
24. Prajapati, J.; Dudhagara, P.; Patel, K. Production of thermal and acid-stable pectinase from Bacillus subtilis strain BK-3: Optimization, characterization, and application for fruit juice clarification. *Biocatal. Agric. Biotechnol.* **2021**, *35*, 102063. [CrossRef]
25. Ahmed, N.E.; El Shamy, A.R.; Awad, H.M. Optimization and immobilization of amylase producedby Aspergillus terreus using pomegranate peel waste. *Bull. Natl. Res. Cent.* **2020**, *44*, 109. [CrossRef]
26. Wang, F.; Terry, N.; Xu, L.; Zhao, L.; Ding, Z.; Ma, H. Fungal laccase production from lignocellulosic agricultural wastes by solid-state fermentation: A review. *Microorganisms* **2019**, *7*, 665. [CrossRef]
27. Maktouf, S.; Neifar, M.; Drira, S.J.; Baklouti, S.; Fendri, M.; Châabouni, S.E. Lemon juice clarification using fungal pectinolytic enzymes coupled to membrane ultrafiltration. *Food Bioprod. Process.* **2014**, *92*, 14–19. [CrossRef]

28. da Câmara Rocha, J.; da Silva Araújo, J.; de Paiva, W.K.V.; Ribeiro, E.S.S.; de Araújo Padilha, C.E.; de Assis, C.F.; dos Santos, E.S.; de Macêdo, G.R.; de Sousa Junior, F.C. Yellow mombin pulp residue valorization for pectinases production by Aspergillus niger IOC 4003 and its application in juice clarification. *Biocatal. Agric. Biotechnol.* **2020**, *30*, 101876. [CrossRef]

29. Asgher, M.; Iqbal, H.M.N.; Irshad, M. Characterization of purified and xerogel immobilized novel lignin peroxidase produced from Trametes versicolor IBL-04 using solid state medium of corncobs. *BMC Biotechnol.* **2012**, *12*, 1–8. [CrossRef]

30. Kumar, P.; Kamle, M.; Singh, J. Biochemical characterization of Santalum album (Chandan) leaf peroxidase. *Physiol. Mol. Biol. Plants* **2011**, *17*, 153–159. [CrossRef]

31. Andriani, A.; Sukorini, A.; Perwitasari, U.Y. Enhancement of laccase production in a new isolated Trametes hirsuta LBF-AA017 by lignocellulosic materials and its application for removal of chemical dyes. *IOP Conf. Ser. Earth Environ. Sci.* **2019**, *308*, 012015. [CrossRef]

32. Khatri, B.P.; Bhattarai, T.; Shrestha, S.; Maharjan, J. Alkaline thermostable pectinase enzyme from Aspergillus niger strain MCAS2 isolated from Manaslu Conservation Area, Gorkha, Nepal. *Springerplus* **2015**, *4*, 488. [CrossRef] [PubMed]

33. Dange, V.; Harke, S. Production and purification of Pectinase by fungal strain in solid-state fermentation using agro-industrial bioproduct. *World J. Microbiol. Biotechnol.* **2018**, *16*, 277–282.

34. Cardinali, A.; Sergio, L.; Di Venere, D.; Linsalata, V.; Fortunato, D.; Conti, A.; Lattanzio, V. Purification and characterization of a cationic peroxidase from artichoke leaves. *J. Sci. Food Agric.* **2007**, *87*, 1417–1423. [CrossRef]

35. Sandri, I.G.; Lorenzoni, C.M.T.; Fontana, R.C.; da Silveira, M.M. Use of pectinases produced by a new strain of Aspergillus niger for the enzymatic treatment of apple and blueberry juice. *LWT Food Sci. Technol.* **2013**, *51*, 469–475. [CrossRef]

36. Osuji, A.C.; Eze, S.O.O.; Osayi, E.E.; Chilaka, F.C. Biobleaching of industrial important dyes with peroxidase partially purified from garlic. *Sci. World J.* **2014**, *2014*, 183163. [CrossRef]

37. Mohamed, S.A.; Abdel-Aty, A.M.; Hamed, M.B.; El-Badry, M.O.; Fahmy, A.S. Ficus sycomorus latex: A thermostable peroxidase. *African J. Biotechnol.* **2011**, *10*, 17532–17545.

38. Yihong, H. Purification and partial characterization of peroxidase from lettuce stems. *African J. Biotechnol.* **2012**, *11*, 2752–2756. [CrossRef]

39. Mall, R.; Naik, G.; Mina, U.; Mishra, S.K. Purification and characterization of a thermostable soluble peroxidase from citrus medica leaf. *Prep. Biochem. Biotechnol.* **2013**, *43*, 137–151. [CrossRef]

40. Geng, Z.; Rao, K.J.; Bassi, A.S.; Gijzen, M.; Krishnamoorthy, N. Investigation of biocatalytic properties of soybean seed hull peroxidase. *Catal. Today* **2001**, *64*, 233–238. [CrossRef]

41. Singh, P.; Prakash, R.; Shah, K. Effect of organic solvents on peroxidases from rice and horseradish: Prospects for enzyme based applications. *Talanta* **2012**, *97*, 204–210. [CrossRef]

42. Chanwun, T.; Muhamad, N.; Chirapongsatonkul, N.; Churngchow, N. Hevea brasiliensis cell suspension peroxidase: Purification, characterization and application for dye decolorization. *AMB Express* **2013**, *3*, 1–9. [CrossRef]

43. Liu, J.Z.; Wang, T.L.; Ji, L.N. Enhanced dye decolorization efficiency by citraconic anhydride-modified horseradish peroxidase. *J. Mol. Catal. B Enzym.* **2006**, *41*, 81–86. [CrossRef]

44. Sofia, P.; Asgher, M.; Shahid, M.; Randhawa, M.A. Chitosan beads immobilized Schizophyllum commune IBL-06 lignin peroxidase with novel thermo stability, catalytic and dye removal properties. *J. Anim. Plant Sci.* **2016**, *26*, 1451–1463.